



## OPEN ACCESS

## EDITED BY

Rachel Collin,  
Smithsonian Tropical Research  
Institute (SI), United States

## REVIEWED BY

Elizabeth Sibert,  
Yale University, United States  
Susumu Ohtsuka,  
Hiroshima University, Japan

## \*CORRESPONDENCE

Alexia Lourtie  
Alexia.Lourtie@umons.ac.be  
Laurent Duchatelet  
Laurent.Duchatelet@uclouvain.be  
Jérôme Delroisse  
Jerome.Delroisse@umons.ac.be

<sup>†</sup>These authors have contributed  
equally to this work

## SPECIALTY SECTION

This article was submitted to  
Marine Biology,  
a section of the journal  
Frontiers in Marine Science

RECEIVED 30 March 2022

ACCEPTED 24 August 2022

PUBLISHED 15 September 2022

## CITATION

Lourtie A, Duchatelet L, Straube N,  
Puozzo N, Grace MA, Naylor GJP and  
Delroisse J (2022) Placoid scales in  
bioluminescent sharks: Scaling their  
evolution using morphology and  
elemental composition.  
*Front. Mar. Sci.* 9:908237.  
doi: 10.3389/fmars.2022.908237

## COPYRIGHT

© 2022 Lourtie, Duchatelet, Straube,  
Puozzo, Grace, Naylor and Delroisse.  
This is an open-access article  
distributed under the terms of the  
[Creative Commons Attribution License  
\(CC BY\)](https://creativecommons.org/licenses/by/4.0/). The use, distribution or  
reproduction in other forums is  
permitted, provided the original  
author(s) and the copyright owner(s)  
are credited and that the original  
publication in this journal is cited, in  
accordance with accepted academic  
practice. No use, distribution or  
reproduction is permitted which does  
not comply with these terms.

# Placoid scales in bioluminescent sharks: Scaling their evolution using morphology and elemental composition

Alexia Lourtie<sup>1,2\*†</sup>, Laurent Duchatelet<sup>1\*†</sup>, Nicolas Straube<sup>3</sup>,  
Nathan Puozzo<sup>2</sup>, Mark A. Grace<sup>4</sup>, Gavin J. P. Naylor<sup>5</sup>  
and Jérôme Delroisse<sup>2\*</sup>

<sup>1</sup>Marine Biology Laboratory, Earth and Life Institute, Université catholique de Louvain - UCLouvain, Louvain-la-Neuve, Belgium, <sup>2</sup>Biology of Marine Organisms and Biomimetics, Research Institute for Biosciences, University of Mons - UMONS, Mons, Belgium, <sup>3</sup>Department of Natural History, University Museum of Bergen, Bergen, Norway, <sup>4</sup>National Oceanic & Atmospheric Administration, Mississippi Laboratories, Southeast Fisheries Science Center, National Marine Fisheries Service, Pascagoula, MS, United States, <sup>5</sup>Florida Museum of Natural History, University of Florida, Gainesville, FL, United States

Elasmobranchs are characterised by the presence of placoid scales on their skin. These scales, structurally homologous to gnathostome teeth, are thought to have various ecological functions related to drag reduction, predator defense or abrasion reduction. Some scales, particularly those present in the ventral area, are also thought to be functionally involved in the transmission of bioluminescent light in deep-sea environments. In the deep parts of the oceans, elasmobranchs are mainly represented by squaliform sharks. This study compares ventral placoid scale morphology and elemental composition of more than thirty deep-sea squaliform species. Scanning Electron Microscopy and Energy Dispersive X-ray spectrometry, associated with morphometric and elemental composition measurements were used to characterise differences among species. A maximum likelihood molecular phylogeny was computed for 43 shark species including all known families of Squaliformes. Character mapping was based on this phylogeny to estimate ancestral character states among the squaliform lineages. Our results highlight a conserved and stereotypical elemental composition of the external layer among the examined species. Phosphorus-calcium proportion ratios (Ca/P) slightly vary from 1.8-1.9, and fluorine is typically found in the placoid scale. By contrast, there is striking variation in shape in ventral placoid scales among the investigated families. Character-mapping reconstructions indicated that the shield-shaped placoid scale morphotype is likely to be ancestral among squaliform taxa. The skin surface occupied by scales appears to be reduced in luminous clades which reflects a relationship between scale coverage and the ability to emit light. In luminous species, the placoid scale morphotypes are restricted to pavement, bristle- and spine-shaped except for the only luminescent somniosid, *Zameus squamulosus*, and the dalatiid *Mollisquama mississippiensis*. These results, deriving from an unprecedented sampling, show extensive morphological diversity in placoid scale shape but little variation in elemental composition among Squaliformes.

## KEYWORDS

dermal denticles, deep-sea sharks, morpho-mapping, scanning electron microscopy, Energy-dispersive X-ray spectrometer (EDX), Dalatiidae, Etmopteridae, Somniosidae

## Introduction

Although deep-sea research is steadily increasing, the mesopelagic and bathyal zones, which extend from 200 to 4,000 meters in depth, remain poorly known and studied (Howell et al., 2021). Abiotic conditions in these environments are extreme, with (i) pressures reaching several hundred atmospheres, (ii) a constant low temperature, (iii) a low concentration of dissolved oxygen, and (iv) an absence of sunlight at depths below 1,000 meters (MacDonald, 1975). Among the diversity of fishes in the deep-sea, various chondrichthyans [i.e., rays (batomorphs), sharks (selachians), and chimaeras] are found (Herring and Morin, 1978; Gage and Tyler, 1992; Herring, 2001). Selachians comprise two major super-orders: (i) the galeomorphs (Galeomorphii) and (ii) the squalomorphs (Squalomorphii) (Naylor et al., 2012; Straube et al., 2015). Within the squalomorphs, the order Squaliformes contains 31 genera and 187 species (Pollerspöck and Straube, 2021). The Squaliform order includes numerous deep-sea sharks and is composed of six families (i) Squalidae, (ii) Centrophoridae, (iii) Dalatiidae, (iv) Somniosidae, (v) Oxyntidae and (vi) Etmopteridae (Figure 1A). Molecular phylogenetic studies show Oxyntidae nested within

Somniosidae (Straube et al., 2010; Naylor et al., 2012; Straube et al., 2015).

Three Squaliforme families contain bioluminescent species, i.e., species able to produce light: the Etmopteridae (Straube et al., 2015; Duchatelet et al., 2020b; Duchatelet et al., 2021a), the Dalatiidae (Claes et al., 2012; Straube et al., 2015; Delroisse et al., 2021; Mallefet et al., 2021; Duchatelet et al., 2021a) and the Somniosidae (Straube et al., 2015; Mallefet et al., 2021). In bioluminescent sharks, the photophores are present within the integument and are located in between the placoid scales (Ohshima, 1911; Hubbs et al., 1967; Claes and Mallefet, 2009; Renwart et al., 2014; Renwart et al., 2015; Mallefet et al., 2021; Duchatelet et al., 2021a). Interestingly, bioluminescent sharks probably have the highest number of photophores within bioluminescent animals (Hubbs et al., 1967; Herring and Morin, 1978). Reif (1985a) suggested an evolutionary trade-off in space occupancy between photophores and placoid scales (i.e., the dermal denticle covering the skin defined as one of the main synapomorphies characterising chondrichthyans) (Applegate, 1967; Deynat, 2014; Lund and Grogan, 2015; Rodríguez-Cabello et al., 2016). In mesopelagic luminous sharks, placoid scale coverage was reduced allowing the coexistence of epidermal photophores and placoid scales in luminescent

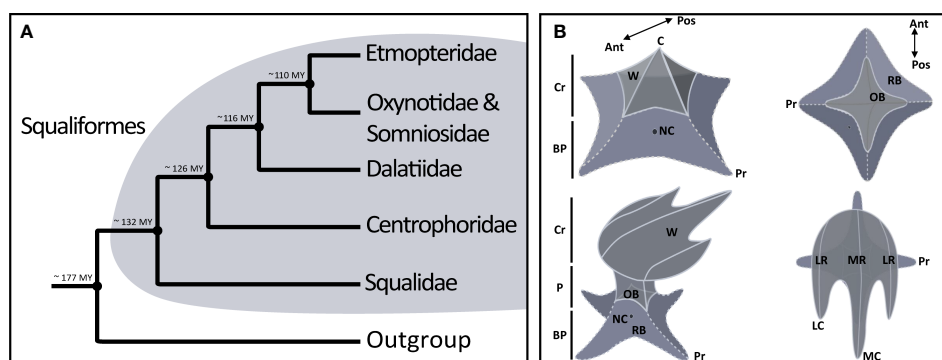


FIGURE 1

Generalised structure of placoid scales with annotated structures in sharks including Squaliformes. (A) Phylogeny of Squaliformes based on Straube et al., 2015, with the estimated divergence times of the families. The divergence shown are corresponding to mean ages.

(B) Schematic representations of a dermal denticle illustrating the morphological terminology: Cr, crown; P, peduncle; R, ridge; LR, lateral ridge; MR, median ridge; OB, observed base; RB, real base; NC, neck-canal; BP, basal plate; C, cusp (LC, lateral cusp and MC, median cusp); Pr, process; W, wing. There is a 2D top view and a 2.5 D lateral view with the anteroposterior orientation (Ant.= Anterior and Pos.= Posterior).

sharks (Reif, 1985b; Ferrón and Botella, 2017). Claes and Mallefet (2009) highlighted different types of placoid scales in luminescent sharks (e.g., pavement-shaped and bristle-shaped). By comparison, non-bioluminescent sharks usually have shield- or leaf-shaped denticles (Compagno, 2001). Recently, two new types of placoid scales were described for the luminescent ventral area of *Zameus squamulosus* and the rostral area of *Dalatias licha* (Duchatelet et al., 2021a; Duchatelet et al., 2021b; Mallefet et al., 2021). Surprisingly (i.e., it appears counterintuitive to the trade-off hypothesis of Reif, 1985a), both species have overlapping shield-shaped placoid scales with light organs embedded in the skin underneath (Straube et al., 2015; Duchatelet et al., 2021a; Duchatelet et al., 2021b; Mallefet et al., 2021). The emitted light is able to pass through the placoid scale (Straube et al., 2015) and the scale might act as a bioluminescence enhancer (Duchatelet et al., 2021a; Duchatelet et al., 2021b). This last hypothetical function could be added to the traditionally described ecological functions of placoid scales which are (i) enhancement of hydrodynamic properties, (ii) defense against parasites, (iii) anti-fouling, (iv) protection against predators, and (v) protection against substrate abrasion (Reif, 1985a; Han et al., 2008; Han and Wang, 2011; Oeffner and Lauder, 2012; Wen et al., 2014; Ferrón et al., 2018; Munther et al., 2018; Feld et al., 2019; Lloyd et al., 2021).

Placoid scales are homologous to gnathostome teeth (Kawasaki et al., 1980; Reif, 1985b; Reif, 1985a; Enax et al., 2012; Enault et al., 2015) and their general morphology and morphogenesis are very similar, as well as their chemical composition (Kawasaki et al., 1980; Reif, 1985a). Chemically, placoid scales are mainly composed of hydroxyapatite crystals interspersed with a dense network of collagen and other proteins such as phospho- and glycoproteins forming a compact structure (Kawasaki et al., 1980; Kawaguchi, 1985; Samuel et al., 1987; Kemp, 1989). Structurally, placoid scales comprise two distinct layers: the dentin and the enameloid (Reif, 1985a; Rodríguez-Cabello et al., 2020). The chemical formula for the enameloid mineral part is  $\text{Ca}_5[\text{PO}_4]_3[\text{OH}]$  (Frank, 1961; Lussi et al., 2015). The Fluorine element can bind to this molecule to form crystals of calcium fluorohydroxyapatite ( $\text{Ca}_5[\text{PO}_4]_3\text{F}$ ) making the structure less prone to demineralisation (Lussi et al., 2015). However, scarce information is available on the elemental composition of placoid scales and no studies have been carried out on deep-sea sharks. Placoid scales exhibit several typical morphological features: a scale base that is not visible externally as it is covered by the tegument, a visible base corresponding to the junction between the placoid scale and the tegument, a peduncle, a crown, wings, ridges, and cusps (Figure 1B; Ebert, 2015; Rodríguez-Cabello et al., 2020). The morphology and arrangement of placoid scales can be species-specific and is often used in species identification (Reif, 1985b; Raschi and Tabit, 1992; Deynat, 2000; Gravendeel et al., 2002; Claes and Mallefet, 2009; Dillon et al., 2017; Ferrón and Botella, 2017; Ankhelyi et al., 2018; Duchatelet et al., 2020a). Intraspecific

variation of placoid scale morphology is observed at different body regions (Duchatelet et al., 2020a; Feichtinger et al., 2021; Gabler-Smith et al., 2021; Naylor et al., 2021) but, within a dedicated body region, the intraspecific variation is low (authors' pers. obs.). Differences - in both morphology and squamation pattern - are often present between two different skin areas (e.g., ventral, dorsal) of an individual (Reif, 1985b; Raschi and Tabit, 1992; Deynat, 2000; Gravendeel et al., 2002; Claes and Mallefet, 2009; Dillon et al., 2017; Ferrón and Botella, 2017; Ankhelyi et al., 2018; Feld et al., 2019; Duchatelet et al., 2020a; Lloyd et al., 2021).

The present work examines the general morphology and distribution pattern as well as the elemental composition of placoid scales from different deep-sea inhabiting Squaliformes. Our study focuses on the ventral skin area that is serving the main function in bioluminescent shark species for countershading (i.e., silhouette cloaking) (Claes et al., 2010; Claes et al., 2014; Duchatelet et al., 2021a).

## Materials and methods

### Sample collection

A total of 33 different shark species were sampled *via* field collecting or in museum collections (Supplementary Table S1). Due to the rarity of some species, only one adult individual was sampled for each species. *Etmopterus spinax* specimens were harvested by longlines in January 2017 during a campaign in the Raunefjord (60°15'54"N; 05°07'46"E; Norway) at 250 m depth. *Etmopterus molleri*, *Heptranchias perlo*, *Squalus mitsukurii*, and *Centrophorus moluccensis* specimens were sampled with an electric fishing rod in November 2017 in the East China Sea near the coast of Sesoko Island in Okinawa (26°28'94"N; 127°41'20"E; Japan) 480 to 510 m depth. *Pristiophorus japonicus*, *Squalus japonicus*, *Squalus brevirostris*, *Etmopterus pusillus*, *Etmopterus brachyurus*, *Etmopterus bigelowi*, *Etmopterus polli*, and *Centroscymnus owstonii* specimens were obtained from the collection of the Churaumi Aquarium of Okinawa. *Etmopterus lucifer*, *Squalus acanthias*, *Etmopterus granulosus*, *Centrophorus squamosus*, *Deania calcea*, *Dalatias licha*, *Scymnodon macracanthus*, and *Oxynotus bruniensis* were collected during the "Chatham survey 2018" campaign (Hoki Survey, Chatham Rise Survey - February 2018 - R/V Tangaroa) off New Zealand. *Zameus squamulosus* specimens were obtained from a collection at the Te Papa Museum in New Zealand. *Squaliolus aliae*, *Trigonognathus kabeyai*, and *Etmopterus splendidus* specimens were collected from industrial fishing vessels operating from the port of Donggang, Taiwan. The first two species were fished with open water nets at depths between 50 and 400 m. *E. splendidus* was obtained by bottom trawling at depths of 300 – 600 m. The holotype (TU 203676; 142.0 mm in total length and 14.6 g in total weight) of *M. mississippiensis* (which represents the only

known specimen of this species) was collected in the central Gulf of Mexico on 4 February 2010 by the NOAA Ship PISCES (survey 7620101001, station 053). The remaining species (*Etmopterus robindsi*, *E. sheikoi*, *Aculeola nigra*, *Isistius brasiliensis*, *Squaliolus laticaudus*, *Centroscyllium nigrum* and *Centroselachus crepidater*) were provided by the Bavarian State Collection of Zoology (Munich, Germany), the Museum für Naturkunde Berlin (Germany) and the National History Museum Paris (France). Living individuals were euthanised according to the ethical regulations of the host country. A ventral skin patch of about 1 cm<sup>2</sup> was dissected from the ventral area located between the two pectoral fins and stored in 90% ethanol until use.

## Scanning electron microscopy (SEM) and microanalyses

For scanning electron microscope observations, ventral skin patches were fixed in Bouin's fluid (saturated aqueous picric acid solution - formalin - glacial acetic acid, 15:5:1, Rai et al., 2016) at room temperature for 24 h, then dehydrated in sequential concentrations of ethanol and dried by the critical-point method using CO<sub>2</sub> as the transition fluid (Renwart et al., 2015; Delroisse et al., 2017, for technical details). Samples were mounted on aluminium stubs, coated with a mix of gold/palladium (40/60) in a sputter coater, and observed with a JEOL JSM 6100 scanning electron microscope. To perform the observation, the sample was placed inside the SEM observation chamber and the working distance (WD) was set up to 10 mm. The voltage was set to 10 kV with average beam width to photographic optimisation. Under these conditions and with a fixed 100 X magnification, three micrographs were made for each skin sample (i.e., technical replicate illustrating three different regions of the sample). Subsequently, three scales were selected inside a random area of the ventral skin sample according to three selection criteria: (i) entire and in good condition (ii) visible as a whole and (iii) oriented to avoid shading effects due to electrons.

Each picture was used for obtaining four datapoints: (i) the maximal distance between the base tips, (ii) the maximal distance between the epidermis and the higher points on the scale (iii) the number of scales under a 100 X magnification and (iv) the percentage of epidermis covered by placoid scale under a 100 X magnification (i.e., scale coverage). Measurements were performed using the Fiji software (Schindelin et al., 2012).

A determination key was created, based on these characteristics, to classify the different placoid scale types (Supplementary Figure S1). To clarify the terminology used in the study, we created a generalised scheme representing the

dermal denticle using the program Adobe Illustrator (Figure 1B). Three main morphotypes are recognised. First, pavement-shaped scales (M1) are the only ones to have a scale's height lower than the scale base's length. The other two morphotypes are differentiated by the presence or absence of a peduncle. The scales without peduncles are classified as bristle/spine-shaped (M2), which are sub-divided into either ("Bristle-shaped", M2a) or ("Spine-shaped", M2b) based on their relative heights. The pedunculated scales are grouped as shield-shaped scales (M3). Depending on the characteristics of the ridges, several sub-categories are defined for type M3. Some shield-shaped scales do not have ridges or show only small ridges, visible on the peduncle (M3a). The others have ridges visible in SEM, which can be divergent (M3b) or running parallel (M3c) (Supplementary Figure S1). SEM data was obtained for all 33 shark species listed in the "sample collection" section. In addition, literature data was used to characterise *Somniosus microcephalus* (Somniosidae) (i.e., 34 investigated species in total) (Castro, 2010).

The elemental composition was analysed using Oxford X-MaxN Energy-dispersive X-ray spectrometer (EDS-EDX) equipped with an 80 mm<sup>2</sup> silicon drift detector (and coupled with the SEM). Acquisition conditions on the SEM were 15 kV, 10 mm working distance and 10 s live time acquisition at approximately 30–40% dead time. The spectra were acquired with an AZtec (Oxford Instrument) EDS data processing software. Two kinds of elemental analyses were performed. First, maps of the general composition are produced for each main element (C, O, F, Na, Mg, Al, P, S, K, Ca). All maps were processed using the AZtec true map function. Second, the elemental composition of three points on the scale and one off-scale point are analysed to determine the elements typically found inside and outside the scale. For each species, skin samples from single individuals were investigated and several technical replicates were performed (i.e., three different points on a scale, for three different scales). Because of the importance of the ratio Ca/P in dental analyses, which are similar in elemental composition to dermal denticles, we included them in this study. An Etmopteridae tooth (*E. molleri*) was used as an external reference for the elemental composition analyses. Descriptive statistics were performed, and the element proportions are expressed as the median/mean values in weight per cent (Wt%) associated with a standard deviation (SD) (median/mean ± SD). To illustrate the variation of the element composition (F, P, Ca, C, O, Na, Mg, Al, S, K, M, N) across the investigated species/families, we performed a principal component analysis (PCA) based on a variance-covariance matrix using PAST 4.02 (Hammer et al., 2001). Descriptive statistics were conducted in the R software package (R Core Team, 2021) using the "ggplot2" Package (Wickham, 2011) and using Prism 9 (GraphPad Software).

## Analyses of character evolution

Initially, a species phylogeny including suitable outgroups based on available DNA sequences of the mitochondrial NADH-ubiquinone oxidoreductase chain 2 (NADH2) was estimated. Used samples are listed in [Supplementary Table S2](#) and were downloaded from Genbank (<https://www.ncbi.nlm.nih.gov/genbank>) and additional sequences were provided by the Chondrichthyan Tree of Life Project (<https://sharkrays.org>). Sequences were subsequently aligned in Geneious<sup>®</sup> 7.1.9 using the MUSCLE sequence aligner (Katoh et al., 2002; Katoh et al., 2005). A maximum likelihood phylogeny was computed using RAxML vers. 8.2.12 (Stamatakis, 2014). We used the general time reversible substitution model with a GAMMA distribution of rate heterogeneity. The phylogeny based on nuclear genes in Straube et al. (2015) was used as backbone tree under RAxML's -g option where the maximum likelihood tree is constrained to the provided backbone topology. Bootstrapping was carried out with 500 replicates and mapped onto the maximum likelihood tree ([Supplementary Figure S2](#)).

In a next step, the maximum likelihood tree was used for the ancestral character state reconstruction for placoid scale morphotypes. Beforehand, the phylogenetic tree (including 43 species) was pruned to match our species sampling for the ancestral character state reconstructions (32 species, [Supplementary Table S2](#)). Ancestral character states were performed in Mesquite v.3.40 (Maddison and Maddison, 2011) using a parsimony model with characters treated as unordered. We based ancestral state reconstructions on the topology of our newly generated phylogeny. Morpho-mapping analyses were performed to estimate placoid scale evolution across the 32 shark species. Three variables were analysed (i) the denticle morphotype, (ii) the coverage percentage of the epidermis with placoid scales (denticle coverage), and (iii) the ability to emit light, i.e., the presence of photophores (see morphological data and corresponding character states matrix in [Supplementary Tables S3, S4](#)). The morphotype character comprises the aforementioned three main character states: (i) pavement-shaped scales (M1), (ii) bristle/spine-shaped scales (M2), which is represented in two subcategories (M2a: bristle-shaped; M2b: spine-shaped) and (iii) shield shaped (M3), subdivided in three categories (M3a: without ridges; M3b: with diverging ridges; M3c: with parallel ridges). The placoid scale coverage, corresponding to the percentage of epidermis overlapped by the placoid scales, was categorised into four-character states: individuals (i) with less than 10% denticle coverage; (ii) with a denticle coverage between 10% and 30%; (iii) with a denticle coverage of 31% to 90% and (iv) with scales covering almost all their epidermis (>90%). In a comparative approach, our sampling includes 34 species (i.e., 33 were sampled), including 20 luminescent species. Two sampled species (*E. robinsi*, *S. mitsukurii*) were not included in the

ancestral character state reconstructions because the NADH Dehydrogenase Subunit 2 sequence data was lacking, and we were not able to clarify their precise phylogenetic position.

## Results

### Phylogeny of Squaliformes

The NADH2 sequence alignment comprises 1044 nucleotide sites. The alignment has 600 distinct patterns and a proportion of gaps and undetermined characters of 0.21%. The tree topology resulting from the maximum likelihood analysis recovers clades as in Straube et al. (2015) due to the backbone tree used for guiding the phylogenetic inference. In summary, Squaliformes are monophyletic, Squalidae are sister to all remaining families where *Squalus* and *Cirrhigaleus* form sister clades. Centrophoridae comprise sister clades *Deania* and *Centrophorus*. The family splits sequentially after Squalidae and is sister to a clade comprising Dalatiidae, Somniosidae (including Oxynotidae) and Etmopteridae. Dalatiidae split in two clades, one comprising *Isistius*, *Dalatis*, and *Mollisquama*, the other *Squaliolus* and *Euprotomicrus*. Somniosidae are sister to Etmopteridae and comprises two major clades representing the *Somniosus* lineage as well as all other somniosid genera also including Oxynotidae. Etmopteridae are split in four clades corresponding to the previously described intrageneric *Etmopterus* clades, i.e., the *E. lucifer* clade, the *E. spinax* clade, the *E. gracilispinis*, and the *E. pusillus* clades ([Supplementary Figure S2](#)).

### External morphology of ventral placoid scales in 34 Squaliformes species

Our analyses, focusing on the ventral placoid scales only, highlight morphological variability among the 34 Squaliformes species ([Figure 2](#), [Supplementary Figures S1, S3](#)).

Different morphotypes are found in the investigated Etmopteridae species. *E. bigelowi*, *E. pusillus*, *E. sheikoi* and *T. kabeyai* have pavement-shaped scales (M1) with an average denticle height and length of 25  $\mu\text{m}$  and 225  $\mu\text{m}$ , respectively. Other Etmopteridae species have bristle/spine-shaped scales (M2) with an average denticle height and length of 275  $\mu\text{m}$  and 100  $\mu\text{m}$ , respectively, subdivided into two subcategories (M2a and M2b). *E. robinsi*, *E. spinax* and *E. brachyurus* have longer scales, assigned to the bristle-shaped morphotype (M2a). *A. nigra*, *C. nigrum*, *E. granulatus*, *E. molleri*, *E. polli* and *E. splendidus* represent the spine-shaped scales (M2b). All Etmopteridae have a low denticle coverage (i.e., percentage of epidermis overlapped by the placoid scales), which cover less than 30% of the epidermis.

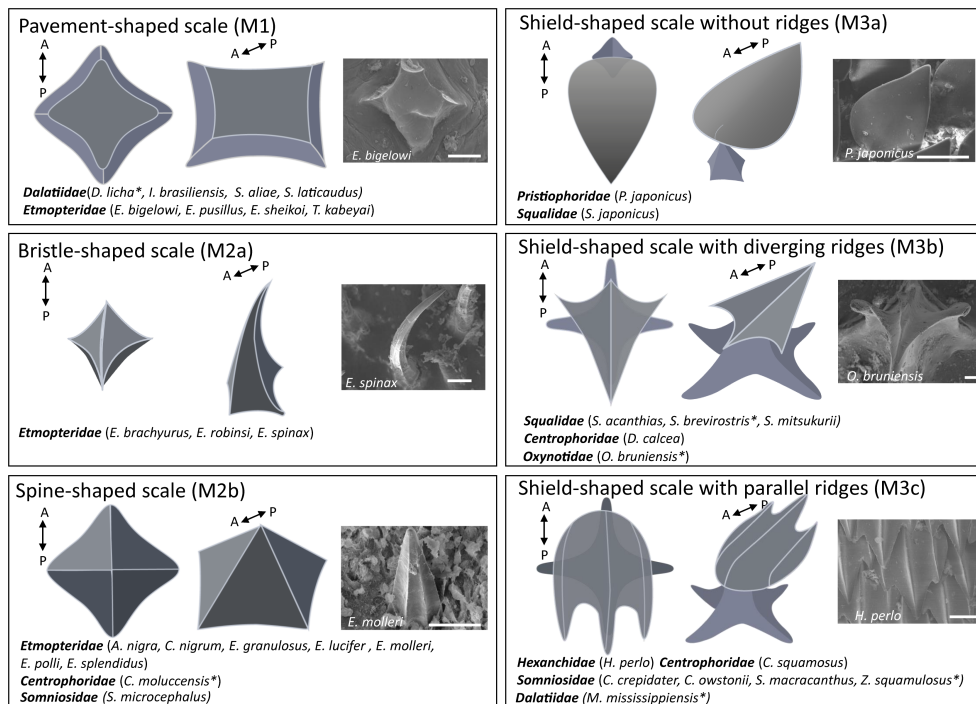


FIGURE 2

Assignment of the ventral placoid scale morphotypes observed in the 34 investigated species. For each morphotype, two schematic representations of the denticle are shown, the left picture represents a 2D top view and the middle picture represents a 2.5 D lateral view with the anteroposterior information (A= Anterior and P= Posterior). The right picture is a typical denticle observed under the scanning electron microscope (SEM). Scale bars: 100  $\mu\text{m}$ . The \* corresponds to the species exhibiting atypical scales within the different morphotypes.

Four species of Dalatiidae (*D. licha*, *I. brasiliensis*, *S. aliae* and *S. laticaudus*) are characterised by pavement-shaped scales (M1) and low denticle coverage (i.e., less than 40% coverage). *I. brasiliensis*, *S. aliae* and *S. laticaudus* have morphologically similar denticles with an average denticle height and length of 25  $\mu\text{m}$  and 250  $\mu\text{m}$ , respectively. However, *D. licha* presents scales formed by large pavement-shaped denticles with a central ridge and bilateral symmetry with an average of 55  $\mu\text{m}$  and 850  $\mu\text{m}$  of denticle height and length (Supplementary Figure S3).

In Centrophoridae, *D. calcea*, *C. squamosus* have shield-shaped scales (M3). *C. moluccensis*, shows scales as assigned to the spine-shaped morphotype (M2b), which is characterised by very similar height and length (300  $\mu\text{m}$  on average). *P. japonicus* and *S. japonicus* have shield-shaped scale, without ridges (M3a).

The Squalidae members *S. mitsukurii*, *S. brevirostris* and *S. acanthias*, the centrophorids *D. calcea* and oxyntid *O. bruniensis* have shield-shaped scales with diverging ridges (M3b). *Oxyntus bruniensis* has a structurally typical M3b morphotype but they present extreme dimensions (height: about 2 cm; base length: about 1 cm). The squalid *S. brevirostris* has atypical M3b scales with rounded extremities and a very small peduncle (Supplementary Figure S3). The last morphotype group the species with shield-shaped scales with

parallel ridges (M3c) with the dalatiid *M. mississippiensis*, the somniosids *Z. squamulosus*, *C. crepidater*, *C. owstonii* and *S. macracanthus*, as well as the centrophorid *C. squamosus* and the hexanchid *H. perlo* (Supplementary Figure S3). *M. mississippiensis* and *Z. squamulosus* were classified in the M3c category because their ridges present a parallelism, but they also appear more complex than the other shield-shaped scales with parallel ridges observed. Secondary ridges are present and form a honeycomb structure (Supplementary Figures S3, S5). The grouping of the two species in this category indicates a morphological similarity but does not mean that the two scale structures are easily comparable or structurally homologous.

## Morphological evolution of ventral placoid scale in Squaliformes

Morpho-mapping analyses were performed to estimate placoid scale evolution across the investigated shark species. Two characteristics were analysed (i) the denticle morphotype (Figure 3) and (ii) the percentage coverage of epidermis by placoid scales (denticle coverage). This last character has been investigated in relation to the bioluminescence abilities of the sharks (Figure 4).

Etmopteridae have different ventral scale morphotypes (i.e., pavement-shaped, spine/bristle-shaped types). The ancestral character state analysis indicates a spine-shaped morphotype (M2b) in the common ancestor of Etmopteridae (Figure 3) as most likely ancestral character state. Pavement-shaped (M1) and bristle-shaped (M2a) denticles would instead correspond to derived characters within the family. The majority of Dalatiidae (*D. licha*, *I. brasiliensis*, *S. aliae* and *S. laticaudus*), with an exception in *M. mississippiensis*, have pavement-shaped denticles (M1) as some Etmopteridae (*E. bigelowi*, *E. pusillus*, *E. sheikoi*, and *T. kabeyai*). The ancestral character state analysis is inconclusive for Dalatiidae. It indicates a pavement-shaped morphotype (M1) or a shield-shaped morphotype with parallel ridges (M3c) as most likely ancestral character state in Dalatiidae.

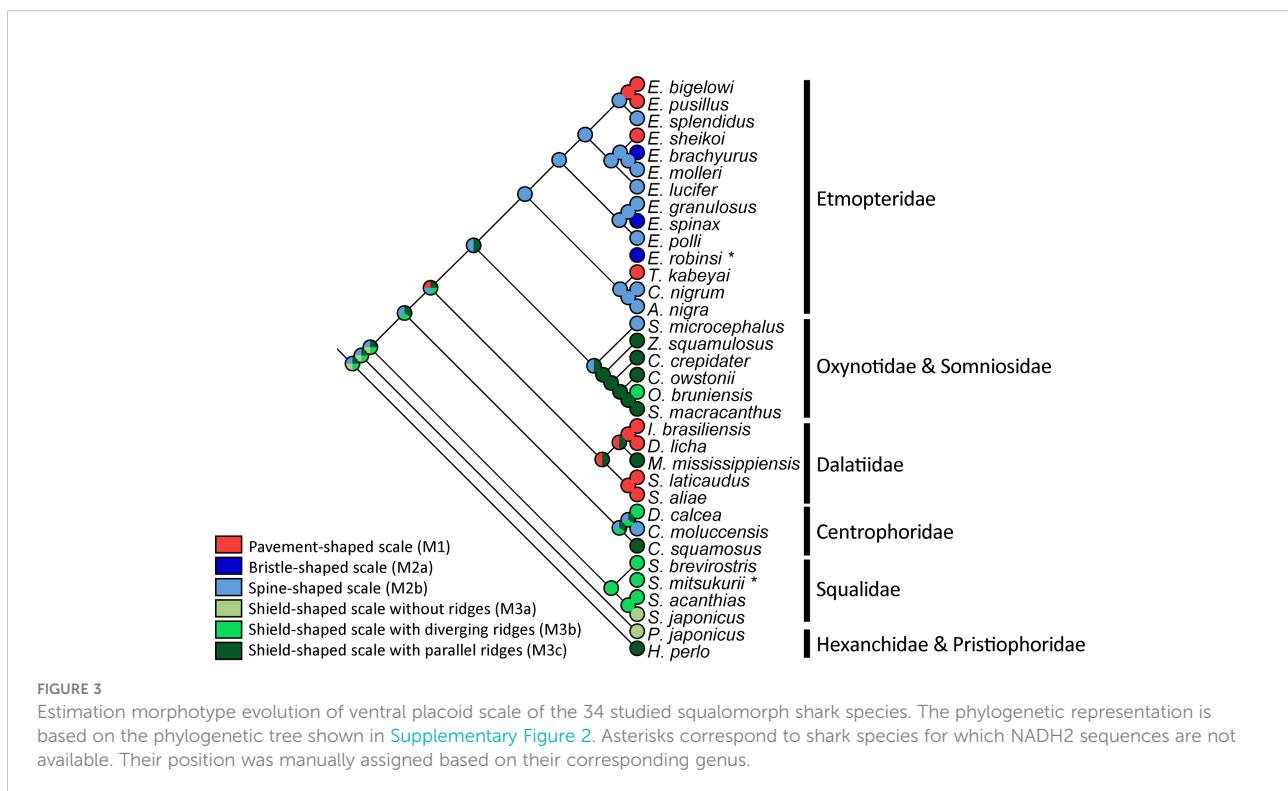
Most investigated species of Somniosidae have shield-shaped scales with parallel ridges (M3c) except for *Somniosus microcephalus* which has spine-shaped scales (M2b). The prickly dogfish, *O. bruniensis* shows a large shield-shaped morphotype with diverging ridges (M3b). Similar to Dalatiidae, the ancestral character state analysis is inconclusive for the clade Oxynotidae and Somniosidae and indicates a spine-shaped morphotype (M2b) or a shield-shaped morphotype with parallel ridges (M3c) as most likely ancestral character state.

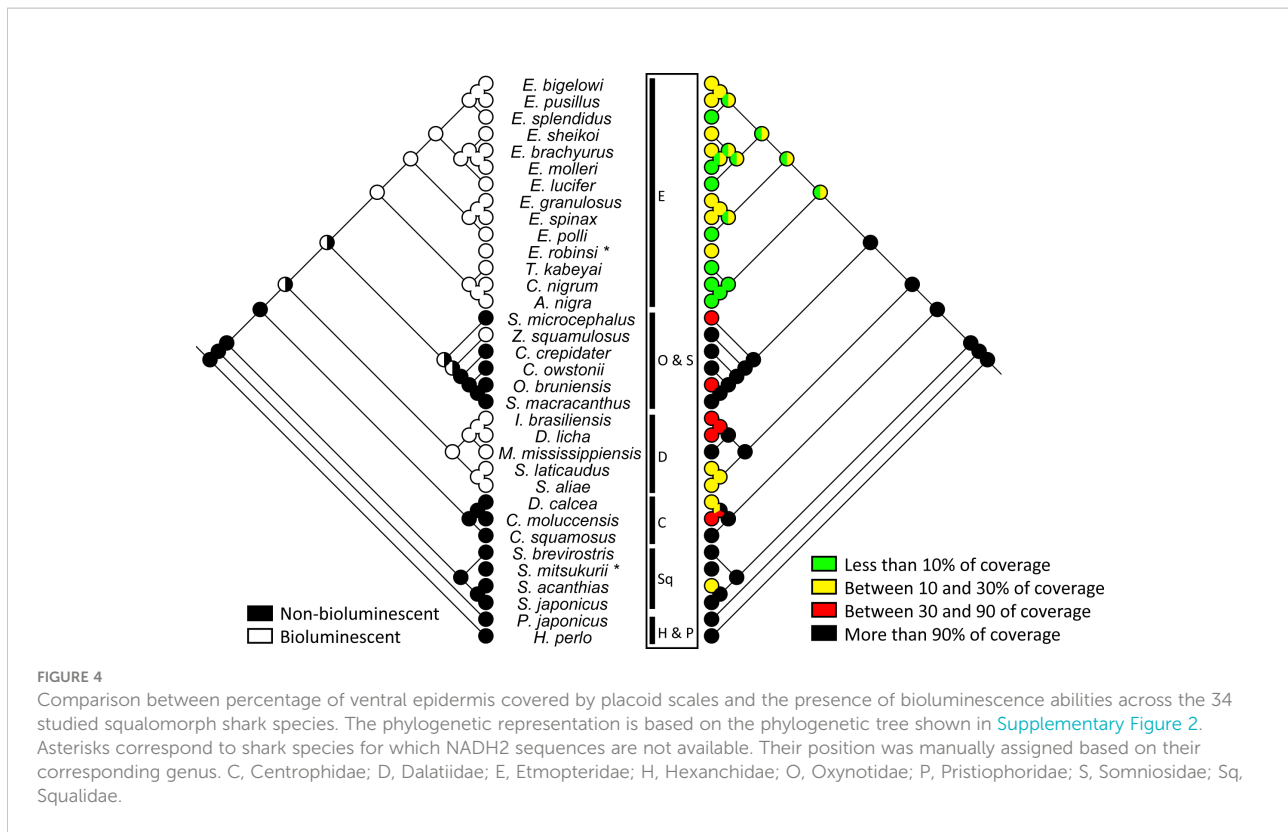
All other families (Squalidae, Centrophoridae, and the outgroup species) show more variability in the ridge's disposition on the shield-shaped denticles. Our parsimony

analyses identified the shield-shaped scale (M3) as ancestral, potentially with parallel ridges (M3c).

The Etmopteridae have the lowest denticle coverage with less than 30% of coverage for all species. The majority of Dalatiidae (i.e., *D. licha*, *I. brasiliensis*, *S. aliae*, *S. laticaudus*) have a higher denticle coverage than the Etmopteridae, ranging from 20% and 50%. A similar coverage is shown in species of Squalidae (*S. acanthias*) and Centrophoridae (*D. calcea*, *C. molluccensis*) analysed herein. All other species investigated in the present study have placoid scales covering 90% or more of their ventral epidermis. Parsimony analyses estimated the ancestral denticle coverage of the common ancestor of Squaliformes to cover the largest part of the ventral epidermis, i.e., 90% or more.

Based on the literature (Haddock et al., 2010; Straube et al., 2015; Duchatelet et al., 2021a; Duchatelet et al., 2021b), we mapped the presence of bioluminescence as character of Etmopteridae and Dalatiidae families, as well as the only known bioluminescent somniosid *Z. squamulosus*, to link it to the denticle coverage (Figure 4). A significant correlation between the scale coverage and the bioluminescence is observed (point-biserial correlation of 0.72): bioluminescent species being generally characterised by a lower scale coverage. In comparison, the scale coverage doesn't appear to be correlated with scale length or height (Pearson correlation of 0.36 and 0.16, respectively). Bioluminescence doesn't appear to be correlated with scale length or height (point-biserial correlation of 0.38 and 0.52), either.





## Elemental compositions of placoid scales in 32 Squalomorph species

The elemental composition of ventral placoid scales and their surrounding epidermis was analysed using Energy-dispersive X-ray Spectroscopy (EDX) coupled with Scanning Electron Microscopy (SEM). EDX analyses gave a rough overview of the main elements observed in the external layer of the placoid scales: carbon (C), oxygen (O), calcium (Ca), phosphorus (P), and to a lesser extent fluorine (F) ([Figure 5A](#); [Supplementary Table S5](#)). Micrographies of elemental composition were generated to identify the elements typically found in the scales ([Figure 5B](#) for *E. molleri*/morphotype M2b; [Supplementary Figure S4](#) for other representative species). On the epidermis, C and O elements were detected in higher proportions relative to the other elements. These elements show important inter-specific and intra-individual variations ( $20.5/23.5 \pm 12\%$  for C,  $45/43 \pm 7\%$  for O) ([Figure 5](#), [Supplementary Table S5](#)). The three other main elements also vary, but to a lesser extent. The proportion of Ca element ranges between  $26.8/24.55 \pm 4.25\%$  in the Etmopterid *E. brachyurus* and  $11.85/12 \pm 1.9\%$  in the Centrophorid *C. squamosus*. The P element proportion ranges between  $13.9/12.3 \pm 2.7\%$  in the Etmopterid *T. kabeyai* and  $7.5/7.2 \pm 1.2\%$  in the Centrophorid *D. calcea*, while it is rather stable in all other taxa. A ratio of the percentage of Ca to P was calculated, and these elements appear

to be correlated ([Figures 5E, F](#); [Supplementary Table S5](#)). The Ca/P ratio variation between the different species is small and about 1.8–1.9. The proportion of F varies in a narrower range of values and ranges between  $1.4/1.7 \pm 0.8\%$  in the Somniosid *Z. squamulosus* and  $5.4/5.4 \pm 0.7\%$  in the Pristiophorid *P. japonicus*. It was not possible to investigate the elemental composition of the scale of the species *M. mississippiensis*.

## Discussion

### Evolution of placoid scale in squaliform deep-sea sharks

Shark squamation is adapted to different lifestyles and ecological niches ([Reif, 1985a](#); [Reif, 1985b](#); [Raschi and Tabit, 1992](#); [Dean and Bhushan, 2010](#); [Chernova and Vorob'eva, 2012](#); [Lang et al., 2012](#); [Fletcher et al., 2014](#); [Ferrón and Botella, 2017](#)). The morphological plasticity of placoid scales is potentially linked to adaptations to ecological conditions ([Reif, 1985b](#); [Reif, 1985a](#); [Raschi and Tabit, 1992](#); [Dean and Bhushan, 2010](#); [Chernova and Vorob'eva, 2012](#); [Ferrón and Botella, 2017](#)). In this study, the phylogenetic distribution of dermal denticle morphotypes (and coverage) was investigated for the first time in squaliform deep-sea sharks. Character mapping was used to test different hypotheses and estimate ancestral character states.

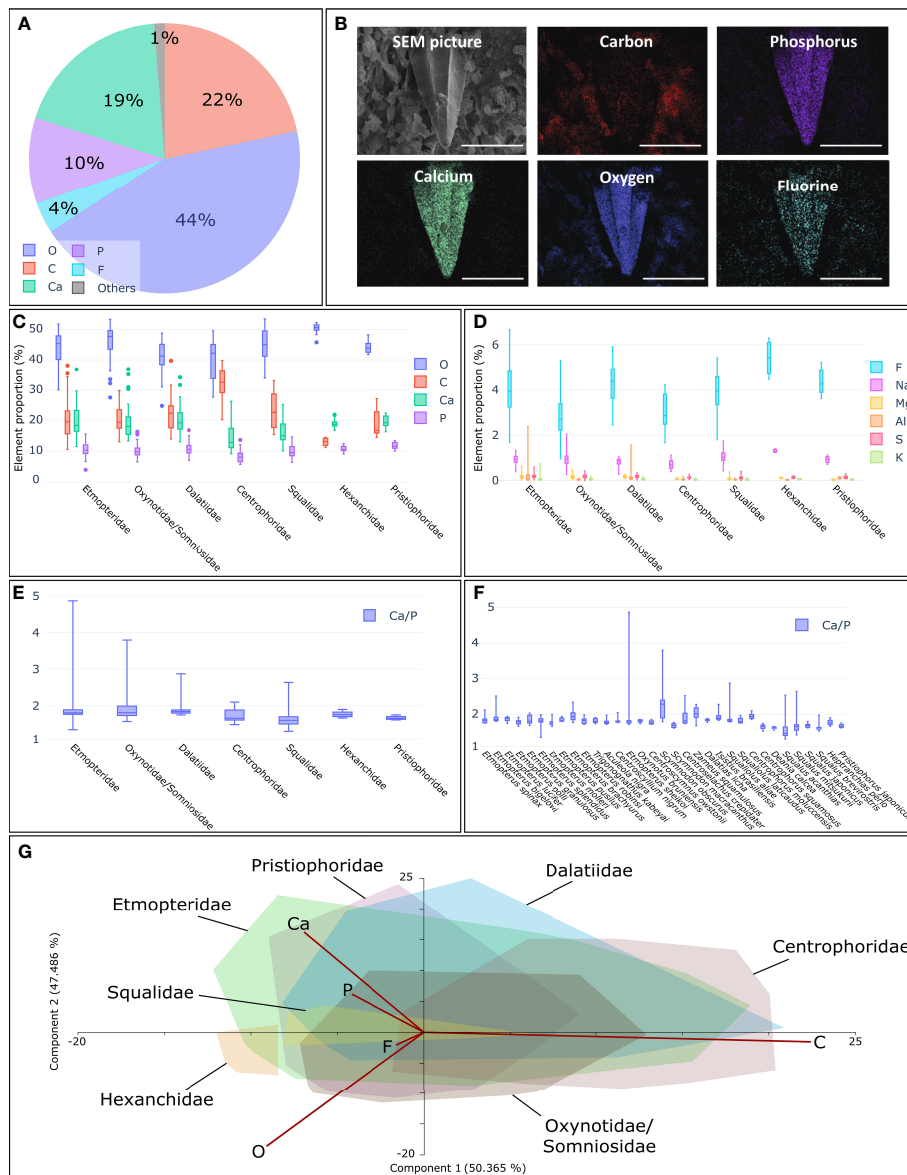


**FIGURE 5** Elemental compositions of ventral placoid scales using EDX-SEM technique. **(A)** Average elemental compositions of the placoid scales of *E. mollerii*. C, carbon; O, oxygen; F, fluorine; Na, sodium; Mg, magnesium; Al, aluminium; P, phosphorus; S, sulphur; K, potassium; Ca, calcium. **(B)** SEM picture of a placoid scale of *E. mollerii* (morphotype M2b) without any EDX analyses and the localisation of the most abundant elements detected by Energy Dispersive X-ray spectrometry (EDX). For every picture, scale = 200µm. **(C)** Elemental proportion (%) of the four main elements (O, C, Ca and P) found on placoid scale clustered by families. **(D)** Elemental proportion (%) of the six other main elements (F, Na, Mg, Al, S and K) found on placoid scale clustered by families. **(E)** Ca/P ratio clustered by families. For C to E, families are *Etmopteridae*, *Oxynotidae/Somniosidae*, *Dalatiidae*, *Centrophoridae*, *Squalidae*, *Hexanchidae* and *Pristiophoridae*. **(F)** Ca/P ratio obtain for the 32 species (except *M. mississippiensis*) targeted by this study. **(G)** PCA illustrating the elemental proportion for all investigated shark families. Only the convex hulls representing the families are shown. Two principal factors extracted from the PCA, PC1 and PC2, accounted for 97.9% of the cumulative variance.

Our parsimony analyses identified the shield-shaped scale (M3) as the most probable ancestral state of ventral placoid scale morphotype among squaliform sharks. Historically, shield-shaped denticles have been assumed to be linked to drag reduction and hydrodynamics functions (Reif, 1985a; Raschi

and Tabit, 1992; Ferrón and Botella, 2017; Feld et al., 2019; Lloyd et al., 2021). During the entire diversification of the Squaliformes, the evolutionary emergence of divergent ridges (M3b) is estimated to have occurred potentially three times independently. The evolutionary emergence of shield-shaped

scales without ridges (M3a) may have occurred twice. Other ventral scale morphotypes are estimated as derived character states, some of which appear to be convergent. The appearance of spine-shaped scales (M2b) seems to coincide with the radiation of the Etmopteridae. The bristle-shaped derived state (M2a) may have appeared at least two times in Etmopteridae. Pavement-shaped scales (M1) potentially evolved four times (once in the Dalatiidae and three times in the Etmopteridae).

The Squaliformes were estimated to have diverged about 177 Ma ago diversifying during the transition from the Lower to the Upper Cretaceous. (Straube et al., 2015). According to the character-mapping analyses, the common ancestor of all 32 species analysed herein had shield-shaped scales, potentially with parallel ridges (M3c). Derived characters may have evolved multiple times independently. The ancestral morphotypes of placoid scales at the base of each squaliform family may be different. In the Dalatiidae, which is estimated to have split from the Etmopteridae/Somniosidae-Oxynotidae clade 116 Ma ago (Straube et al., 2015), the morphotype could be either shield-shaped with parallel ridges (M3c) or pavement-shaped (M1). This latter character state is the most frequent type in extant species of this family (except for *M. mississippiensis*). Within Etmopteridae, which split from the Somniosidae/Oxynotidae clade about 110 Ma ago (Straube et al., 2015), different morphotypes are observed. Most species have spine-shaped scales (M2b), which is assumed to be the ancestral scale type of this family. Bristle-shaped (M2a) and pavement-shaped scales (M1) are estimated to be derived character states within this family.

Species belonging to the bioluminescent Etmopteridae and the majority of Dalatiidae have ventral dermal denticles potentially adapted to facilitate functional ventral bioluminescence. The ventral placoid scale morphology of Etmopteridae can vary depending on the species between spine-shaped morphotype (M2b), pavement-shaped denticles (M1) and the bristle-shaped morphotype (M2a). The majority of Dalatiidae (*D. licha*, *I. brasiliensis*, *S. aliae* and *S. laticaudus*) have pavement-shaped denticles (M1) which could be analogous to the pavement-shaped scales of some Etmopteridae (*E. bigelowi*, *E. pusillus*, *E. sheikoi* and *T. kabeyai*). However, all these scale types have something in common: their distribution results in a small percentage of denticle coverage ventrally allowing coexistence with bioluminescent organs located in the skin. A clear space trade-off between ventral skin photophores and denticles is observed in Etmopteridae. A higher level of denticle coverage is observed in Dalatiidae and the single known bioluminescent Somniosid for which the bioluminescence function is supposed to be limited to countershading. In these two families, the denticle coverage can reach up to 90% (defined as the ancestral character state in Squaliforms) (Figure 3).

Our results support a scenario where a first diversification of non-luminescent squaliforms is characterised by the ancestral M3c denticle morphotype and later evolution of derived

morphotypes facilitating bioluminescence, which is estimated to have emerged in sharks during the diversification of Dalatiidae, Somniosidae/Oxynotidae and Etmopteridae during the transition from the Lower to the Upper Cretaceous (Straube et al. 2015). Although bioluminescence seems to perfectly correlate with a low denticle coverage (mainly in Etmopteridae and most Dalatiidae), two bioluminescent sharks are characterised by a high ventral denticle coverage: *Z. squamulosus* (Somniosidae) and *M. mississippiensis* (Dalatiidae). Both species show a third, entirely different type of shield-shaped denticle with additional honeycomb structures (See for *M. mississippiensis*, Supplementary Figures S3, S5). In *Z. squamulosus*, the denticle appears translucent to luminescence (Duchatelet et al., 2021b). This alternative scale organisation and morphology may represent a by-passing of the trade-off etmopterids and other dalatiid species encounter, where denticles are assumed to compete in space with photophores. In *M. mississippiensis*, ventral photophore aggregations are mentioned for the only specimen observed to date (Grace et al., 2019). Also, numerous dark spots (assumed to be photophores) were mentioned around denticle pedicles and found on the body (Grace et al., 2015; Grace et al., 2019). However, conclusive histology was not possible due to the freezing and thawing of tissue (Julien Claes, pers. comm.). *M. mississippiensis* also has translucent denticles but the light transmissivity has not yet been investigated. A dark area is present in the central part of the scale and is corresponding to the pedicle that anchors into the dermis (Supplementary Figure S5). Further analyses are needed to discuss the potential functional link between these placoid scales and the bioluminescence. It is important to state that the correlation we highlighted between the presence of bioluminescence and the low denticle coverage is not necessarily corresponding to a causative relationship. Alternative hypotheses related to other ecological features (e.g., paucity of food, resource allocations) of these organisms might be related to the specific structures of the dermal denticles in bioluminescent species.

All non-bioluminescent species present shield-shaped denticles, except for *C. moluccensis* (spine-shaped scales). The majority of Somniosidae analysed herein with the exception of *S. microcephalus* (M2a type scales), is equipped with shield-shaped scales with parallel ridges (M3c), a character that also appears as the ancestral state in this shark family. The Oxynotid *O. bruniensis* shows a large shield-shaped morphotype with diverging ridges (M3b). All other families (Squalidae, Centrophoridae and the outgroup species) show more variability on the ridges disposition on the shield-shaped denticles. Shield-shaped denticles can therefore be an advantage for deep-sea sharks, for example serving hydrodynamic functions, which may explain why this placoid scale type is widespread within Squalomorph sharks.

Based on the ventral coverage estimations, the evolution of less denticle coverage allowing for coexistence of denticles and

photophores, could have evolved in Etmopteridae and Dalatiidae independently. The Etmopteridae are estimated to have undergone adaptive radiations in a period of intense modifications in the marine environment, including the deep-sea (Fordyce, 1977; Straube et al., 2010; Claes et al., 2015; Straube et al., 2015). The diversification of *Etmopterus*, the genus showing most complex bioluminescence functions today, was likely rapid and may have been additionally fuelled by the establishment of the circum-antarctic current at the beginning of the Oligocene (Kennett et al., 1974; Fordyce, 1977; Lawver and Gahagan, 2003; Straube et al., 2010; Straube et al., 2015). As such, the pavement-shaped scales occurring in Dalatiidae and some species of Etmopteridae could have been convergently evolved, however bristle and spine-shaped scale type (M2a and b) are specific to the Etmopteridae.

## Elemental composition of ventral placoid scales in deep-sea sharks

Various authors hypothesised that the elemental composition of placoid scales may vary due to biological functions, as it is the case for teths (Murray, 1936; Hennemann, 2001; Riede, 2004). Our EDX analyses highlighted five main elements: C, O, Ca, P and F. C element is found mostly on the epidermis, while Ca, P and F are found almost exclusively on the surface of the placoid scales. Considering these element proportions is interesting because resources in F, Ca or P within mesopelagic and bathyal environments are limited (Gage and Tyler, 1992; Herring, 2001; Ifremer, 2015). Oxygen (O) is present on all samples. This general elemental distribution was conserved in all samples. The O and C element proportions are sometimes high in a single placoid scale. Previous studies have shown that fast swimming sharks produce a nano-layer of mucus that covers their placoid scales to improve their hydrodynamics (Dean and Bhushan, 2010; Lang et al., 2012; Bixler and Bhushan, 2013; Luo, 2015). If such a nano-layer is present in the species studied herein as well, it could influence our elemental composition analyses despite performing various rinsing steps during sample preparation.

While the elemental proportions could vary within the same placoid scale or among species (particularly for Ca and P elements), the Ca/P ratio is homogeneous within placoid scales (ranging from 1.42 to 2.28 for median values per species, from 1.60 to 1.80, median values per family) (Figure 5) and similar to the Ca/P ratio of the *E. molleri* tooth (median value of 1.46, data not shown). They are also similar to that of human dental enamel (Frank, 1961; Lussi et al., 2015). The latter ranges between 1.67 and 2.0 (Murray, 1936; Frank, 1961; Sánchez-Quevedo et al., 1998; Arnold and Gaengler, 2007; Lussi et al., 2015).

The F signal varies in the same value ranges for the different species and all their percentages had low values (global average

value of 3.77 for all investigated species, in comparison the *E. molleri* tooth F proportion was 3.11 on average). The relative amount of fluorine in the upper layer of the placoid scales would therefore be relatively constant and conserved during evolution. The presence of this element results in more resistant and less soluble denticles in the surrounding environment (Lussi et al., 2015). The placoid scales are sometimes described as “non-growing structures” because their span of growth is limited and so they are only replaced when they are too damaged or when they fall out (Reif, 1985a; Reif, 1985b; Kemp, 1989; Helfman et al., 2009; Rodríguez-Cabello et al., 2020). Premature destruction or surface damage of these structures would not allow them to perform their functions and renewal should therefore be faster.

## Conclusion

Our study, based on an unprecedented sampling of squalomorph sharks, sheds light on the evolution of the extant morphological diversity and relative homogeneity of the elemental composition of ventral placoid scales in Squaliformes for the first time.

Our sampling highlights the presence of a typical ventral squamation type in most bioluminescent species, with comprising pavement-shaped, spine-shaped, or bristle-shaped placoid scales scarcely located on the epidermis. However, two bioluminescent species, *Z. squamulosus* and *M. mississippiensis*, have a different kind of squamation, with shield-shaped placoid scales almost fully covering the epidermis. For *Z. squamulosus*, a previous study shows that this scale type is translucent and allows the emitted light to pass through the scale (Duchatelet et al., 2021b). Our results suggest that this morphology serves for additional functionality hitherto not associated with the functions of placoid scales.

Our analyses estimate the ancestral ventral morphotypes of Squaliform placoid scales to be a shield-shaped scale (as observed in most extant sharks). Other morphotypes are derived from this ancestral state. Squamation that would allow coexistence with photophores possibly evolved three times independently in luminescent families Etmopteridae, Dalatiidae and Somniosidae. Ancestral denticles of Etmopteridae are estimated to have a spine-shaped morphotype, a state that is highly preserved in many extant species. Conversely, the pavement-shaped morphotype is widely present in Dalatiidae, but also present in some Etmopteridae. However, the Dalatiidae *M. mississippiensis* and the only Somniosidae known to be bioluminescent, *Z. squamulosus*, show a third ventral scale morphotype, with shield-shaped denticles with honeycomb structures.

All dermal denticles appear to have a very similar chemical composition of their external layer. The elements mostly detected on placoid scales are oxygen, carbon, phosphorus,

calcium, and fluorine. The chemical composition seems to be conserved in Squaliformes belonging to mesopelagic and bathyal systems, regardless of the morphological characteristics of the scales or other ecological or biological characteristics of the different species of sharks.

## Data availability statement

The original contributions presented in the study are included in the article/[Supplementary Material](#). Further inquiries can be directed to the corresponding authors.

## Ethics statement

Ethical review and approval were not required for this study. The shark specimens were either captured as bycatch by local fishermen or from Museum collections.

## Author contributions

AL, LD, and JD performed, analysed and interpreted the SEM pictures. AL and JD performed morpho-mapping, and statistical analyses. AL, JD, and LD performed the first draft manuscript. LD and JD collected and gathered tissue samples. NS provided samples and performed phylogenetic analyses. AL, JD, and NP prepared the figures. NP created schematics of the [Figures 1A, 2](#). JD and LD supervised the work. MG, and GN provided molecular data for the phylogenetic analyses and contributed to the manuscript revision. JD coordinated the preparation of the publication with all co-authors. All authors read and approved the final manuscript.

## Funding

AL is supported by a doctoral grant from the “Fonds de la Recherche Scientifique” (FRIA/F.R.S.-FNRS, Belgium). LD is a postdoctoral researcher from the Catholic University of Louvain. JD is postdoctoral researcher from the F.R.S.–FNRS.

## Acknowledgments

The authors would like to thank T. Sorlie from the Espregrennd Marine Biological Station (University of Bergen, Norway), Dr. K. Sato, Deputy Director-General of the Okinawa Churaumi Aquarium, Dr. T. Tomita, and the

husbandry people from the Okinawa Churaumi Aquarium, Drs. D. Stevens and R. O’Driscoll from the Te papa in New Zealand (Hoki Survey, Chatham Rise Survey – February 2018 & 2020 - R/V Tangaroa) for the help provided during the field samplings and the collection samplings of sharks. We acknowledge Prof. J. Mallefet (UCLouvain, Belgium) for constant support. We also thank Dr. H.-C. Ho from the National Museum of Marine Biology and Aquarium (Taiwan), Dr. B. Séret from the National History Museum of Paris (France), and Drs. J. M. Claes and N. Pinte from the “Université catholique de Louvain” – UCLouvain for the shark sample collections and advice. We deeply thank Dr. H. L. Bart from Tulane University Biodiversity Research Institute for sending us skin of the holotype of *M. mississippiensis*. This study is the contribution of BRC 391 of the Biodiversity Research Center (UCLouvain) from the Earth and Life Institute – Biodiversity (ELIV) and the “Centre Inter-universitaire de Biologie Marine” (CIBIM).

## Conflict of interest

The authors declare that the research was conducted in the absence of any commercial or financial relationships that could be construed as a potential conflict of interest.

## Publisher’s note

All claims expressed in this article are solely those of the authors and do not necessarily represent those of their affiliated organizations, or those of the publisher, the editors and the reviewers. Any product that may be evaluated in this article, or claim that may be made by its manufacturer, is not guaranteed or endorsed by the publisher.

## Supplementary material

The Supplementary Material for this article can be found online at: <https://www.frontiersin.org/articles/10.3389/fmars.2022.908237/full#supplementary-material>

### SUPPLEMENTARY FIGURE 1

Determination key for the observed ventral morphotypes. \* Most of the scales are overlapping, which prevents direct observation of the peduncles.

### SUPPLEMENTARY FIGURE 2

Maximum likelihood phylogeny of squalomorph sharks based on mitochondrial NADH-ubiquinone oxidoreductase chain 2 (NADH2) gene under a GTR + Gamma model using RAxML ([Stamatakis, 2014](#)). Analysed specimens are listed in [Supplementary Table 2](#). Bootstrap

values (500 replicates) are indicated at each node. The phylogeny based on nuclear genes in Straube et al. (2015) was used as backbone tree under RAxML's -g option where the maximum likelihood tree is constrained to the provided backbone topology.

#### SUPPLEMENTARY FIGURE 3

Ventral placoid scale micrographs of the different studied species at constant magnification (X100). For all micrographs, scale = 400  $\mu\text{m}$ . The color code indicates the families to which the individuals belong. Red: Centrophoridae; Blue: Dalatiidae; Green: Etmopteridae; Yellow: Hexanchidae and Pristiophoridae; Purple: Oxynotidae and Somniosidae; Orange: Squalidae. For *C. squamosus* and *S. macrocanthus*, a lower magnification image (X90 and X65) was added in the upper left corner, because the entire scale was not visible at X100 magnification. For *C. nigrum*, a higher magnification photograph (X700) was also added.

#### SUPPLEMENTARY FIGURE 4

SEM picture of ventral placoid scales corresponding to the different morphotypes and Energy Dispersive X-ray spectrometry (EDX) maps highlighting the most abundant elements. (A) Placoid scale of *E. bigelowi* (pavement-shaped; M1). (B) Placoid scale of *E. spinax* (bristle-shaped; M2a). (C) Placoid scale of *P. japonicus* (shield-shaped without ridges; M3a). (D) Placoid scale of *O. bruniensis* (shield-shaped with diverging ridge; M3b). (E) Placoid scale of *H. perlo* (shield-shaped with parallel ridge; M3c).

#### SUPPLEMENTARY FIGURE 5

Ventral placoid scale of *M. mississippiensis* illuminated from below. (A) Scale present on the tegument, (B) an isolated placoid scale. Scales = 150  $\mu\text{m}$ .

#### SUPPLEMENTARY TABLE 1

Specimen collection data. The table includes the taxonomic information (family, species), the sampling site, the collection ID, the collection depth, the sampling method, and the collection date.

#### SUPPLEMENTARY TABLE 2

List of the species investigated for the Squalomorph phylogeny reconstruction including GenBank accession numbers for the NADH Dehydrogenase Subunit 2 sequences and the corresponding tissue sample numbers.

#### SUPPLEMENTARY TABLE 3

Raw data for the morphological analyses (scale height, scale length, number of visible scales under a magnification of X100, scale coverage).

#### SUPPLEMENTARY TABLE 4

Character state matrix used during the Mesquite analyses for the 33 studied shark species. Morphotype: pavement-shaped (M1), bristle-shaped (M2a), spine-shaped (M2b), shield-shaped without ridge (M3a), shield-shaped with diverging ridges (M3b), shield-shaped with parallel ridges (M3c); surface coverage: 1 – less than 10% of coverage, 2 – between 10 and 30% of coverage, 3 – between 30 and 90% of coverage, 4 – more than 90% of coverage.

#### SUPPLEMENTARY TABLE 5

Raw data obtained using EDX elemental proportion analyses for C= carbon, O= oxygen, F= fluorine, Na= sodium, Mg= magnesium, Al= aluminium, P= phosphorus, S= sulphur, K= potassium, Ca= calcium. For all species, three measurements represent the elemental composition analysed on the placoid scale, and one measurement was performed outside the scale (on the tegument).

## References

- Ankhelyi, M. V., Wainwright, D. K., and Lauder, G. V. (2018). Diversity of dermal denticle structure in sharks: Skin surface roughness and three-dimensional morphology. *J. Morphol.* 279, 1132–1154. doi: 10.1002/jmor.20836
- Applegate, S. P. (1967). "A survey of shark hard parts," in *Sharks, skates and rays*. Eds. P. W. Gilbert, R. F. Mathewson and D. P. Rall (Baltimore: John Hopkins Press).
- Arnold, W. H., and Gaengler, P. (2007). Quantitative analysis of the calcium and phosphorus content of developing and permanent human teeth. *Ann. Anat.* 189, 183–190. doi: 10.1016/j.aanat.2006.09.008
- Bixler, G. D., and Bhushan, B. (2013). Fluid drag reduction with shark-skin riblet inspired microstructured surfaces. *Adv. Funct. Mater.* 23, 4507–4528. doi: 10.1002/adfm.201203683
- Castro, J. I. (2010). *The sharks of north America* (New York, NY: Oxford University Press).
- Chernova, O. F., and Vorob'eva, E. I. (2012). Polymorphism of the surface sculpture of placoid scales of sharks (Selachomorpha, elasmobranchii). *Dokl. Biol. Sci.* 446, 316–319. doi: 10.1134/S0012496612050067
- Chondrichthyan Tree of Life (2016) *Chondrichthyan tree of life*. Available at: <https://sharksrays.org/> (Accessed May, 2022).
- Claes, J. M., Aksnes, D. L., and Mallefet, J. (2010). Phantom hunter of the fjords: camouflage by counterillumination in a shark (Etmopterus spinax). *J. Exp. Mar. Biol. Ecol.* 388 (1–2), 28–32. doi: 10.1016/j.jembe.2010.03.009
- Claes, J. M., Ho, H.-C., and Mallefet, J. (2012). Control of luminescence from pygmy shark (*Squaliolus aliae*) photophores. *J. Exp. Biol.* 215, 1691–1699. doi: 10.1242/jeb.066704
- Claes, J. M., and Mallefet, J. (2009). "Bioluminescence of sharks: first synthesis," in *Bioluminescence in focus - a collection of illuminating essays*. Ed. V. Meyer Rochow (Thiruvananthapuram: Research Signpost), 51–65.
- Claes, J. M., Nilsson, D.-E., Mallefet, J., and Straube, N. (2015). The presence of lateral photophores correlates with increased speciation in deep-sea bioluminescent sharks. *R. Soc. Open Sci.* 2, 150219. doi: 10.1098/rsos.150219
- Claes, J. M., Partridge, J. C., Hart, N. S., Garza-Gisholt, E., Ho, H.-C., Mallefet, J., et al. (2014). Photon hunting in the twilight zone: visual features of mesopelagic bioluminescent sharks. *PLoS One* 9, 1–13. doi: 10.1371/journal.pone.0104213
- Compagno, L. J. V. (2001). Sharks of the world. an annotated and illustrated catalogue of shark species known to date. *FAO Fisher. Sympos.* 125, 249.
- Dean, B., and Bhushan, B. (2010). Shark-skin surfaces for fluid-drag reduction in turbulent flow: a review. *Phil. Trans. R. Soc. A* 368, 4775–4806. doi: 10.1098/rsta.2010.0201
- Delroisse, J., Duchatelet, L., Flammang, P., and Mallefet, J. (2021). Photophore distribution and enzymatic diversity within the photogenic integument of the cookie-cutter shark *Isistius brasiliensis* (Chondrichthyes: Dalatiidae). *Front. Mar. Sci.* 8. doi: 10.3389/fmars.2021.627045
- Delroisse, J., Ullrich-Lüter, E., Blaue, S., Eeckhaut, I., Flammang, P., and Mallefet, J. (2017). Fine structure of the luminous spines and luciferase detection in the brittle star *Amphiura filiformis*. *Zoologischer Anzeiger* 269, 1–12. doi: 10.1016/j.jcz.2017.05.001
- Deynat, P. (2000). Les Denticules myrmécoides, un nouveau caractère diagnostique pour les rajidae (Chondrichthyes, batoidea). *Annales Des. Sci. Naturelles - Zoologie Biologie Animale* 21, 65–80. doi: 10.1016/S0003-4339(00)00106-4
- Deynat, P. (2014). *La peau des requins et des raies* Vol. 7 (Monaco: Institut océanographique Fondation Albert 1er, Prince de Monaco).
- Dillon, E. M., Norris, R. D., and O'Dea, A. (2017). Dermal denticles as a tool to reconstruct shark communities. *Mar. Ecol. Prog. Ser.* 566, 117–134. doi: 10.3354/meps12018
- Duchatelet, L., Claes, J. M., Delroisse, J., Flammang, P., and Mallefet, J. (2021a). Glow on sharks: state of the art on bioluminescence research. *Oceans* 2, 822–842. doi: 10.3390/oceans2040047
- Duchatelet, L., Marion, R., and Mallefet, J. (2021b). A third luminous shark family: confirmation of luminescence ability for *Zameus squamulosus* (Squaliformes; somniosidae). *Photochem. Photobiol.* 97, 739–744. doi: 10.1111/php.13393

- Duchatelet, L., Moris, V. C., Tomita, T., Mahillon, J., Sato, K., Behets, C., et al. (2020a). The megamouth shark, *Megachasma pelagios*, is not a luminous species. *PLoS One* 15, e0242196. doi: 10.1371/journal.pone.0242196
- Duchatelet, L., Sugihara, T., Delroisse, J., Koyanagi, M., Rezoahazy, R., Terakita, A., et al. (2020b). From extraocular photoreception to pigment movement regulation: a new control mechanism of the lanternshark luminescence. *Sci. Rep.* 10, 10195. doi: 10.1038/s41598-020-67287-w
- Ebert, D. A. (2015). Deep-sea cartilaginous fishes of the southeastern Atlantic ocean. *FAO Species Catalogue Fishery Purposes* 264. doi: www.fao.org/3/i4619e/i4619e.pdf
- Enault, S., Guinot, G., Koot, M. B., and Cuny, G. (2015). Chondrichthyan tooth enameloid: past, present, and future. *Zool. J. Linn. Soc.* 174, 549–570. doi: 10.1111/zoj.12244
- Enax, J., Prymak, O., Raabe, D., and Epple, M. (2012). Structure, composition, and mechanical properties of shark teeth. *J. Struct. Biol.* 178, 290–299. doi: 10.1016/j.jsb.2012.03.012
- Feichtinger, I., Adnet, S., Cuny, G., Guinot, G., Kriwet, J., Neubauer, T. A., et al. (2021). Comment on “An early Miocene extinction in pelagic sharks. *Science* 374 (6573), Article abk0632. doi: 10.1126/science.abk0632
- Feld, K., Kolborg, A. N., Nyborg, C. M., Salewski, M., Steffensen, J. F., and Berg-Sørensen, K. (2019). Dermal denticles of three slowly swimming shark species: microscopy and flow visualization. *Biomimetics* 4, 38. doi: 10.3390/biomimetics4020038
- Ferrón, H. G., and Botella, H. (2017). Squamation and ecology of thelodonts. *PLoS One* 12, e0172781. doi: 10.1371/journal.pone.0172781
- Ferrón, H. G., Paredes-Aliaga, M. V., Martínez-Pérez, C., and Botella, H. (2018). Bioluminescent-like squamation in the galeomorph shark *Apristurus ampliceps* (Chondrichthyes: Elasmobranchii). *Contrib. Zool.* 87, 187–196. doi: 10.1163/18759866-08703004
- Fletcher, T., Altringham, J., Peakall, J., Wignall, P., and Dorrell, R. (2014). Hydrodynamics of fossil fishes. *Proc. R. Soc. B: Biol. Sci.* 281, 20140703. doi: 10.1098/rspb.2014.0703
- Fordyce, R. E. (1977). The development of the circum-antarctic current and the evolution of the mysticeti (mammalia: Cetacea). *Palaeogeogr. Palaeoclimatol. Palaeoecol.* 21, 265–271. doi: 10.1016/0031-0182(77)90038-4
- Frank, R. M. (1961). Conceptions nouvelles concernant l’email et sa genèse. *Arch. Oral Biol.* 4, 29–33. doi: 10.1016/0003-9969(61)90074-7
- Gabler-Smith, M. K., Wainwright, D. K., Wong, G. A., and Lauder, G. V. (2021). Dermal denticle diversity in sharks: novel patterns on the interbranchial skin. *Integr. Organism Biol.* 3 (1), obab034. doi: 10.1093/iob/obab034
- Gage, J. D., and Tyler, P. A. (1992). *Deep-sea biology: a natural history of organisms at the deep-sea floor* (Cambridge: Cambridge University Press).
- Grace, M. A., Doosey, M. H., Bart, H. L., and Naylor, G. J. P. (2015). First record of *Mollisquama* sp. (Chondrichthyes: Squaliformes: Dalatiidae) from the Gulf of Mexico, with a morphological comparison to the holotype description of *Mollisquama parini* Dolganov. *Zootaxa* 3948 (3). doi: 10.11646/zootaxa.3948.3.10
- Grace, M. A., Doosey, M. H., Denton, J. S. S., Naylor, G. J. P., Bart, H. L. Jr., and Maisey, J. G. (2019). A new Western north Atlantic ocean kitefin shark (Squaliformes: Dalatiidae) from the gulf of Mexico. *Zootaxa* 4619, 109–120. doi: 10.11646/zootaxa.4619.1.4
- Gravendeel, R., Van Neer, W., and Brinkhuizen, D. (2002). An identification key for dermal denticles of rajidae from the north Sea. *Int. J. Osteoarchaeol.* 12, 420–441. doi: 10.1002/oa.645
- Haddock, S. H. D., Moline, M. A., and Case, J. F. (2010). Bioluminescence in the sea. *Annu. Rev. Mar. Sci.* 2, 443–493. doi: 10.1146/annurev-marine-120308-081028
- Hammer, O., Harper, D. A. T., and Ryan, P. D. (2001). Past: Paleontological statistics software package for education and data analysis. *Palaeontologia Electronica* 4 (1), 4.
- Han, X., and Wang, J. (2011). A novel method for fabrication of the biomimetic shark-skin coating. *Adv. Mat. Res.* 239–242, 3014–3017. doi: 10.4028/www.scientific.net/AMR.239-242.3014
- Han, X., Zhang, D., Li, X., and Li, Y. (2008). Bio-replicated forming of the biomimetic drag-reducing surfaces in large area based on shark skin. *Chin. Sci. Bull.* 53, 1587. doi: 10.1007/s11434-008-0219-3
- Helfman, G. S., Collette, B. B., Facey, D. E., and Bowen, B. W. (2009). *The diversity of fishes: biology, evolution, and ecology*. 2nd ed. (Malden: Blackwell Science).
- Hennemann, R. M. (2001). *Sharks & rays: elasmobranch guide of the world* (Frankfurt: Hollywood Import & Export, Inc).
- Herring, P. (2001). *The biology of the deep ocean* (Oxford: Oxford University Press).
- Herring, P., and Morin, J. (1978). *Bioluminescence in fishes* (London: Academic Press).
- Howell, K. L., Hilário, A., Allcock, A. L., Bailey, D., Baker, M., Clark, M. R., et al. (2021). A decade to study deep-sea life. *Nat. Ecol. Evol.* 5, 265–267. doi: 10.1038/s41559-020-01352-5
- Hubbs, C. L., Iwai, T., and Matsubara, K. (1967). External and internal characters, horizontal and vertical distribution, luminescence, and food of the dwarf pelagic shark *Euprotomicrus bispinnatus*. *Bull. Scripps Inst. Oceanogr.* 10, 1–64.
- Ifremer (2015). *Abysses, les mystères des profondeurs. émission en direct de l’Ifremer et dossier océans et climat*. Ifremer, France
- Katoh, K., Kuma, K. I., Toh, H., and Miyata, T. (2005). MAFFT version 5: improvement in accuracy of multiple sequence alignment. *Nucleic Acid Res.* 33, 511–518. doi: 10.1093/nar/gki198
- Katoh, K., Misawa, K., Kuma, K. I., and Miyata, T. (2002). MAFFT: a novel method for rapid multiple sequence alignment based on fast Fourier transform. *Nucleic Acid Res.* 30, 3059–3066. doi: 10.1093/nar/gkf436
- Kawaguchi, T. (1985). Chemical nature of collagen in the placoid-scale dentine of the blue shark, *Prionace glauca* L. *Arch. Oral Biol.* 30, 385–390. doi: 10.1016/0003-9969(85)90064-0
- Kawasaki, H., Kawaguchi, T., Yano, T., Fujimura, S., and Yago, M. (1980). Chemical nature of proteins in the placoid scale of the blue shark, *Prionace glauca* L. *Arch. Oral Biol.* 25, 313–320. doi: 10.1016/0003-9969(80)90040-0
- Kemp, N. E. (1989). “The phosphatic mode of calcification in ontogeny and phylogeny of the integument and skeleton of vertebrates,” in *Origin, evolution, and modern aspects of biomineralization in plants and animals*. Ed. R. E. Crick (Boston: Springer US), 237–249.
- Kennett, J. P., Houtz, R. E., Andrews, P. B., Edwards, A. R., Gostin, V. A., Hajos, M., et al. (1974). Development of the circum-antarctic current. *Science* 186, 144–147. doi: 10.1126/science.186.4159.144
- Lang, A., Habegger, M. L., and Motta, P. (2012). “Shark skin drag reduction,” in *Encyclopedia of nanotechnology*. Ed. B. Bhushan (Dordrecht: Springer Netherlands), 2394–2400.
- Lawler, L. A., and Gahagan, L. M. (2003). Evolution of Cenozoic seaways in the circum-Antarctic region. *Palaeogeogr. Palaeoclimatol. Palaeoecol.* 198, 11–37. doi: 10.1016/S0031-0182(03)00392-4
- Lloyd, C. J., Peakall, J., Burns, A. D., Keevil, G. M., Dorrell, R. M., Wignall, P. B., et al. (2021). Hydrodynamic efficiency in sharks: the combined role of riblets and denticles. *Bioinspir. Biomim.* 16, 046008. doi: 10.1088/1748-3190/abf3b1
- Lund, R., and Grogan, E. (2015). “Origin and relationships of early chondrichthyans,” in *Biology of sharks and their relatives*. Eds. J. C. Carrier, J. A. Musick and M. R. Heithaus (New York: CRC Press), 3–29.
- Luo, Y. (2015). Recent progress in exploring drag reduction mechanism of real sharkskin surface: a review. *J. Mech. Med. Biol.* 15, 1. doi: 10.1142/S0219519415300021
- Lussi, A., Hellwig, E., and Kmíček, J. (2015). Fluorures – comment agissent-ils exactement? *Rev. Mensuelle Suisse d’Odontostomatologie* 122, 3.
- MacDonald, A. G. (1975). *Physiological aspects of deep-sea biology* (Cambridge: Cambridge University Press).
- Maddison, W., and Maddison, D. (2011). *Mesquite: a modular system for evolutionary analysis, version 2.75*.
- Mallefet, J., Stevens, D. W., and Duchatelet, L. (2021). Bioluminescence of the largest luminous vertebrate, the kitefin shark, *Dalatias licha*: first insights and comparative aspects. *Front. Mar. Sci.* 8. doi: 10.3389/fmars.2021.633582
- Munther, M., Palma, T., Angeron, I. A., Salari, S., Ghassemi, H., Vasefi, M., et al. (2018). Microfabricated placoid scale-inspired surfaces for antifouling applications. *Appl. Surf. Sci.* 453, 166–172. doi: 10.1016/j.apsusc.2018.05.030
- Murray, M. M. (1936). The chemical composition of teeth. *Biochem. J.* 30, 1567–1571.
- Naylor, G. J. P., Caira, J. N., Jensen, K., Rosana, K. A. M., Straube, N., and Lakner, C. (2012). “Elasmobranch phylogeny: a mitochondrial estimate based on 595 species,” in *Biology of sharks and their relatives, second edition*. Eds. J. C. Carrier, J. A. Musick and M. R. Heithaus (New York: CRC Press), 31–56.
- Naylor, G. J. P., de Lima, A., Castro, J. I., Hubbell, G., and de Pinna, M. C. C. (2021). Comment on “An early Miocene extinction in pelagic sharks. *Science* 374 (6573), Article abj8723. doi: 10.1126/science.abj8723
- Offner, J., and Lauder, G. V. (2012). The hydrodynamic function of shark skin and two biomimetic applications. *J. Exp. Biol.* 215, 785–795. doi: 10.1242/jeb.063040
- Ohshima, H. (1911). Some observations on the luminous organs of fishes. *J. Coll. Sci. Imp. Univ. Tokyo* 27, 1–25. doi: 10.1002/jez.1402590102
- Pollerspöck, J., and Straube, N. (2021). “Bibliography database of living/fossil sharks, rays and chimaeras (Chondrichthyes: Elasmobranchii, holocephali) - list of valid extant species; list of described extant species; statistic”. Available at: [https://shark-references.com/images/meine\\_bilder/downloads/List\\_species\\_03\\_2021.pdf](https://shark-references.com/images/meine_bilder/downloads/List_species_03_2021.pdf) (Accessed November 17, 2021).
- Rai, R., Bhardwaj, A., and Verma, S. (2016). Tissue fixatives: A review. *Int. J. Pharmaceutics Drug Anal* 4 (4), 183–187.
- Raschi, W., and Tabit, C. (1992). Functional aspects of placoid scales: a review and update. *Mar. Freshw. Res.* 43, 123–147. doi: 10.1071/mf920123

- R Core Team (2021). *R: A language and environment for statistical computing* (Vienna, Austria: R Foundation for Statistical Computing). Available at: <https://www.R-project.org/>.
- Reif, W.-E. (1985a). Functions of scales and photophores in mesopelagic luminescent sharks. *Acta Zool.* 66, 111–118. doi: 10.1111/j.1463-6395.1985.tb00829.x
- Reif, W.-E. (1985b). *Squamation and ecology of sharks*. Frankfurt am Main, Germany: Courier Forschungsinstitut Senckenberg.
- Renwart, M., Delroisse, J., Claes, J. M., and Mallefet, J. (2014). Ultrastructural organization of lantern shark (*Etmopterus spinax* linnaeus 1758) photophores. *Zoomorphology* 133, 405–416. doi: 10.1007/s00435-014-0230-y
- Renwart, M., Delroisse, J., Flammang, P., Claes, J. M., and Mallefet, J. (2015). Cytological changes during luminescence production in lanternshark (*Etmopterus spinax* linnaeus 1758) photophores. *Zoomorphology* 134, 107–116. doi: 10.1007/s00435-014-0235-6
- Riede, K. (2004). *Global register of migratory species: from global to regional scales: final report of the R&D-projekt 808 05 081* (Bonn Germany: Federal Agency for Nature Conservation).
- Rodríguez-Cabello, C., González-Pola, C., and Sánchez, F. (2016). Migration and diving behavior of *Centrophorus squamosus* in the NE atlantic. combining electronic tagging and argo hydrography to infer deep ocean trajectories. *Deep Sea Res. Part I Oceanogr. Res. Pap.* 115, 48–62. doi: 10.1016/j.dsr.2016.05.009
- Rodríguez-Cabello, C., Pérez, M., and Grasa, I. (2020). Taxonomic research on *Deania calcea* and *Deania profundorum* (Family: Centrophoridae) in the cantabrian Sea (Northeast Atlantic) with comments on *Deania hystricosa*. *Reg. Stud. Mar. Sci.* 37, 101321. doi: 10.1016/j.rsma.2020.101321
- Samuel, N., Bessem, C., Bringas, P. J., and Slavkin, H. C. (1987). Immunochemical homology between elasmobranch scale and tooth extracellular matrix proteins in *Cephaloscyllium ventriosum*. *J. Craniofac. Genet. Dev. Biol.* 7, 371–386.
- Sánchez-Quevedo, M. C., Nieto-Albano, O. H., García, J. M., Gómez de Ferraris, M. E., and Campos, A. (1998). Electron probe microanalysis of permanent human enamel and dentine. a methodological and quantitative study. *Histol. Histopathol.* 13, 109–113. doi: 10.14670/HH-13.109
- Schindelin, J., Arganda-Carreras, I., Frise, E., Kaynig, V., Longair, M., Pietzsch, T., et al. (2012). Fiji: an open-source platform for biological-image analysis. *Nat. Methods* 9, 676–682. doi: 10.1038/nmeth.2019
- Stamatakis, A. (2014). RAxML version 8: a tool for phylogenetic analysis and post-analysis of large phylogenies. *Bioinformatics* 30 (9), 1312–1313. doi: 10.1093/bioinformatics/btu033
- Straube, N., Iglésias, S. P., Sellos, D. Y., Kriwet, J., and Schlieven, U. K. (2010). Molecular phylogeny and node time estimation of bioluminescent lantern sharks (Elasmobranchii: Etmopteridae). *Mol. Phylogenet. Evol.* 56, 905–917. doi: 10.1016/j.ympev.2010.04.042
- Straube, N., Li, C., Claes, J. M., Corrigan, S., and Naylor, G. J. P. (2015). Molecular phylogeny of squaliformes and first occurrence of bioluminescence in sharks. *BMC Evol. Biol.* 15, 162. doi: 10.1186/s12862-015-0446-6
- Wen, L., Weaver, J. C., and Lauder, G. V. (2014). Biomimetic shark skin: design, fabrication and hydrodynamic function. *J. Exp. Biol.* 217, 1656–1666. doi: 10.1242/jeb.097097
- Wickham, H. (2011). ggplot2. *WIREs Comp. Stat.* 3, 180–185. doi: 10.1002/wics.147